



## Magnetic field and performance analysis of a tubular permanent magnet linear synchronous motor applied in elevator door system\*

Xiao LIU<sup>†</sup>, Yun-yue YE, Zhuo ZHENG<sup>†‡</sup>, Qin-fen LU

(School of Electrical Engineering, Zhejiang University, Hangzhou 310027, China)

<sup>†</sup>E-mail: mrluixiao@yahoo.com.cn; jediz@163.com

Received July 25, 2007; revision accepted Nov. 5, 2007; published online Mar. 8, 2008

**Abstract:** A novel elevator door driven by tubular permanent magnet linear synchronous motor (TPMLSM) is presented. This TPMLSM applies axial magnet array topology of the secondary rod, air-cored armature windings and slotless structure of the forcer to improve the stability of the thrust. The influence of two major dimensions, the pitch and radius of the permanent magnet (PM), on magnetic field was studied and the best values were given by the finite element analysis (FEA). The magnetic field, back EMF and thrust of the motor were analyzed and the PM size was optimized to reduce the harmonic components of the magnetic field and improve the performance of the motor. Predicted results are validated by the experiment. It is shown that the performance of the motor and the novel elevator door system is satisfying.

**Key words:** Elevator door system, Tubular permanent magnet linear synchronous motor (TPMLSM), Finite element analysis (FEA)

doi:10.1631/jzus.A071408

Document code: A

CLC number: TM351; TM359.4; TM383.4+2

### INTRODUCTION

Traditionally, the elevator door is driven by a rotary motor and some complex mechanisms, such as gears, cranks, and chains, which transform the rotary motion into linear motion. This kind of drive mode is indirect. The efficiency of the whole system is low, and the dynamic performance is not satisfying. A new elevator door driven directly by a linear induction motor (LIM) is proposed to take the place of traditional rotary motor (Zhou *et al.*, 2006). The transmission mechanism is taken off, and thus the cost of manufacturing is reduced. However, there are also some problems with the LIM-driven elevator door system. The air gap of the LIM is usually designed large to avoid friction between the primary and secondary, so the efficiency is not highly improved, and the acoustic noise caused by LIM is

another major weakness (Zhou *et al.*, 2006). So the LIM-driven elevator door is not widely applied.

In this paper, a novel elevator door driven by a tubular permanent magnet linear synchronous motor (TPMLSM) is presented. This novel TPMLSM-driven elevator door system has the advantages of the LIM-driven system. The elevator door is driven directly by TPMLSM and the mechanism of the door is largely simplified, the manufacturing cost is reduced, and the efficiency is greatly improved, the response speed is high and the acoustic noise is low. The excellent performance of the TPMLSM-driven elevator door system may greatly change the door-driving motor manufacturing.

### TOPOLOGY OF MOTOR

The topology of TPMLSM is sketched in Fig.1, where only three windings are given. In practice, the number of windings should be determined by the actual requirement.

<sup>‡</sup> Corresponding author

\* Project (No. 50607016) supported by the National Natural Science Foundation of China

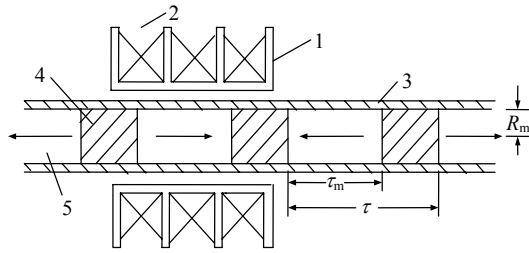


**Fig.1 Topology of the tubular permanent magnet linear synchronous motor (TPMLSM).**  $R_m$ : PM outside radius,

$\tau_m$ : PM pole pitch,  $\tau$  pole pitch

1: Winding frame; 2: Windings; 3: Stainless steel tube; 4: Permanent magnets; 5: Pole-pieces

The motor consists of the forcer and the secondary rod. The forcer is mainly made up of armature windings and the winding frame. The frame is made with non-magnetic material by injection molding. The three-phase air windings are directly wound in the slots of the winding frame.

The secondary rod has an axial magnet array topology (Wang *et al.*, 2001; 2004; Bianchi *et al.*, 2001; 2003; Lu *et al.*, 2005; 2006). The permanent magnets (PMs), which are made of NdFeB N42SH, are magnetized axially, and two opposite polar PMs are spaced by the pole-pieces made of ferromagnetic material. All the PM and pole-pieces are surrounded by a stainless steel tube, the main functions of which are to support and protect the PM and pole-pieces.

Although TPMLSM with Halbach magnet array may get a more sinusoidal magnetic field (Zhu *et al.*, 2000; Jang *et al.*, 2003), it is not easy to magnetize the PM to optional direction as designed and the cost is much higher than that in axial magnet array. Motor with axial magnet array also has a good performance and could be manufactured easily with much lower cost. So the axial magnet structure is chosen.

There is a bearing in each end cover of the forcer. The bearings are made of special alloy material which are durable and wear-resistant. The inside diameter of the bearing is a little bit smaller than the winding frame to avoid the friction between the frame and the secondary rod and reduce the friction force, when the concentricity of the forcer and the rod cannot be guaranteed in mounting.

As the forcer is air-cored, the cogging force could be totally eliminated. So the thrust force would be more stable than that of the iron-cored motor, and the stability of the elevator door in uniform-velocity

motion would be improved. At the meantime, the mass and inertia of the forcer are reduced (Lu *et al.*, 2005; 2006), which makes the motor have better performance in the accelerated and decelerated motion. The air-cored structure also reduces the power loss and the acoustic noise (Zhao *et al.*, 2006).

## FINITE ELEMENT ANALYSIS OF MOTOR

### Magnetic field distribution

Considering the axial symmetry of the TPMLSM, the motor could be simplified to a 2D axial symmetry model in cylindrical coordinate. The following assumptions are made during the analysis: (1) The current density distributes uniformly in the conductor; (2) The hysteresis effect and eddy effect are ignored. The distribution of the magnetic line is shown in Fig.2.

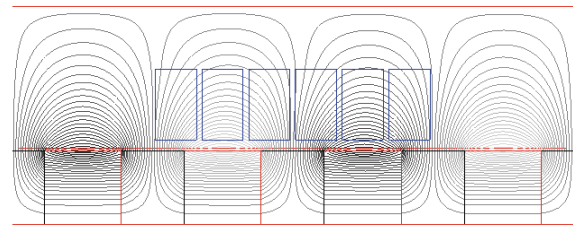


**Fig.2 Distribution of the magnetic line**

For the TPMLSM with axial magnet array, there are three key dimensions for the secondary rod: pole pitch  $\tau$ , PM pole pitch  $\tau_m$  and PM outside radius  $R_m$  (Marignetti and Scarano, 1999; 2002; Bianchi, 2000; Bianchi *et al.*, 2001; Wang *et al.*, 1999; 2001; 2003). The influence of these three key dimensions on the magnetic field distribution could be analyzed by FEA.

Firstly, keep the dimension of  $\tau$  and  $R_m$ , just change the ratio of  $\tau_m/\tau$ . Taking the ratio  $\tau_m/\tau=0.3$  for example, the distributions of the radial magnetic flux density component  $B_r$  at different radial positions are shown in Fig.3. Obviously, at the position closer to the secondary rod, the magnitude of the magnetic flux density is larger, but the distribution waveform is more non-sinusoidal. The average value of the radial magnetic flux density  $B_{ravg}$  is calculated and plotted with a sinusoidal waveform in Fig.4. Comparing the two waveforms in Fig.4, the distribution of the average magnetic flux density is not a sinusoidal curve,

and the harmonic components account for a great proportion. By Fourier analysis on the average magnetic flux density distribution curve, the harmonic components of the magnetic field could be obtained. The magnitudes of the fundamental and harmonic components  $B_{rn}$  are plotted in Fig.5.

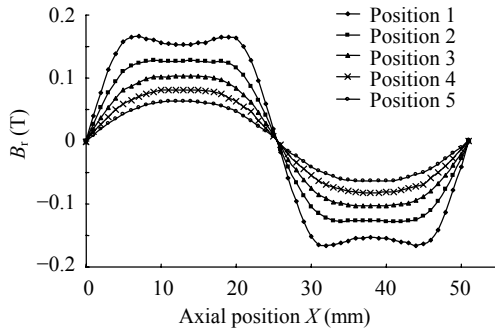


Fig.3 Distributions of the radial magnetic flux density components at different radial positions when  $\tau_m/\tau=0.3$

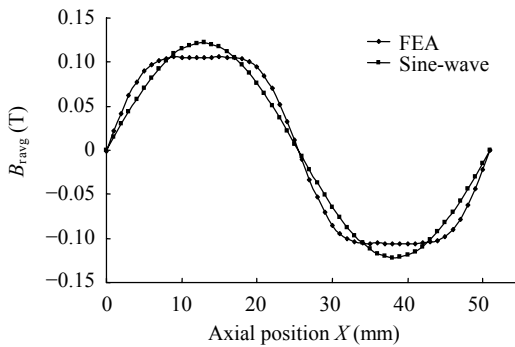


Fig.4 Distribution of the average radial magnetic flux density when  $\tau_m/\tau=0.3$

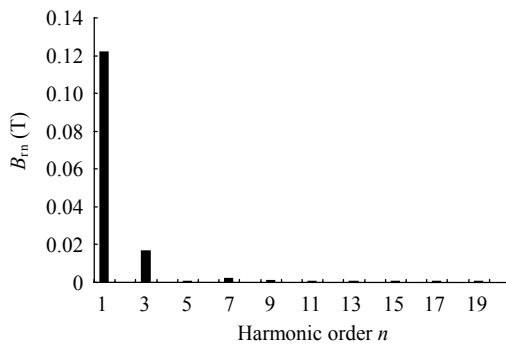


Fig.5 Magnitude of the fundamental and harmonic components when  $\tau_m/\tau=0.3$

As shown in Fig.5, the third-order harmonic component is high, about 13.78% of the fundamental component. Ninth- and above ninth-order harmonic components are too small to be considered.

Similarly, distributions of the magnetic flux density with different ratios of  $\tau_m/\tau$  are analyzed. Magnitude of the fundamental component and proportion of the high-order harmonic components are listed in Table 1.

Table 1 Magnitude of the fundamental component and proportion of the high-order harmonic components with different ratios of  $\tau_m/\tau$

$\tau_m/\tau$	Fundamental (T)	Harmonic components proportion (%)			
		3rd order	5th order	7th order	9th order
0.30	0.1218	13.78	0.48	1.51	0.95
0.40	0.1437	8.26	2.55	1.47	0.57
0.45	0.1535	5.20	3.27	1.15	0.33
0.50	0.1620	2.12	3.52	0.67	0.25
0.55	0.1696	0.97	3.46	0.29	0.33
0.60	0.1775	4.55	2.89	0.13	0.39
0.65	0.1822	6.80	2.27	0.25	0.44
0.70	0.1874	9.55	1.24	0.24	0.55
0.80	0.1949	13.96	1.08	0.38	0.59

Obviously, magnitude of the fundamental component increases as the ratio of  $\tau_m/\tau$  increases, and the distribution of the magnetic flux density is more sinusoidal when the ratio is within 0.45~0.60.

Then, keeping  $\tau_m$  and  $\tau$ , and changing the ratio of  $R_m/\tau$ , the influence of  $R_m$  on the magnetic flux density distribution could be analyzed. Table 2 shows the FEA results with different ratios of  $R_m/\tau$ .

Table 2 Magnitude of the fundamental component and proportion of the high-order harmonic components with different ratios of  $R_m/\tau$

$R_m/\tau$	Fundamental (T)	Harmonic components proportion (%)			
		3rd order	5th order	7th order	9th order
0.30	0.1219	1.56	3.43	0.28	0.31
0.45	0.1696	0.97	3.46	0.29	0.33
0.50	0.1770	0.83	3.53	0.28	0.30
0.55	0.1833	0.69	3.60	0.24	0.23
0.80	0.2411	0.56	3.45	0.29	0.28
1.00	0.2662	0.42	3.49	0.35	0.33

The ratio of  $R_m/\tau$  mainly influences the fundamental component, and the harmonic components change little when the ratio of  $R_m/\tau$  changes. Considering the cost of the PM, the ratio should not be too large. Generally, it is appropriate to choose the ratio within the range of 0.4~0.7.

Based on FEA of the magnetic field, the three key optimized dimensions could be determined, as listed in Table 3. The following analyses are all based on the model with these dimensions.

**Table 3 Key design dimensions of the motor**

Parameter	Value
PM pole pitch $\tau_m$ (mm)	14.03
Pole pitch $\tau$ (mm)	25.50
PM outside radius $R_m$ (mm)	13.00
$\tau_m/\tau$	0.55
$R_m/\tau$	0.51

### Back EMF and thrust force

The no-load back EMF of the motor could be easily obtained as the distribution of magnetic flux density is analyzed. Fig.6 shows the no-load back EMF ( $E$ ) waveform with only one pole pair windings model at the velocity of 51 mm/s. The magnitude is about 0.26 V.

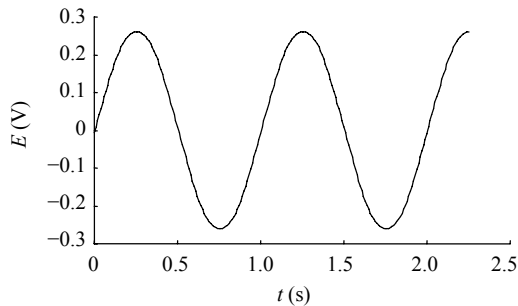


**Fig.6 No-load back EMF per pole at the velocity of 51 mm/s**

The thrust force per pole is calculated by FEA, and the calculated results with different currents are shown in Table 4. As there is no ferromagnetic material in the forcer, the magnetic field would not be saturated. So the ratio of thrust force to current is constant, and the motor has a good variable speed characteristic.

**Table 4 Thrust force calculated by FEA with different currents**

Current (A <sub>pk</sub> )	Thrust force (N)	Current (A <sub>pk</sub> )	Thrust force (N)
0.5	3.875	2.0	15.500
1.0	7.744	2.5	19.355
1.5	11.615	3.0	23.231

## EXPERIMENTAL RESULTS

Prototype of the motor and the elevator door device on which the experimental test is carried out is shown in Fig.7. Table 5 shows the motor specification. FEA and experimental results of the no-load back EMF waveforms are shown in Fig.8. Comparing these two waveforms, the experimental back EMF is 6.54% larger than the FEA value. Fig.9 shows the FEA and experimental results of the thrust force  $F$  with different currents, and the experimental results are also larger than the FEA results. The largest relative error is about 6.22%.



**Fig.7 Prototype of the motor and the elevator door**

**Table 5 Specification of the TPMLSM applied in the elevator door**

Parameter	Value
Number of pole pairs	8
Number of phases	3
Forcer size (mm×mm×mm)	67×67×510
Forcer inner diameter (mm)	29
Secondary rod length (mm)	1000
Secondary rod outer diameter (mm)	28
Back EMF constant (V <sub>pk</sub> /m/s)	43.47
Thrust force constant (N/A <sub>pk</sub> )	65.20
Maximum acceleration (m/s <sup>2</sup> )	61.125

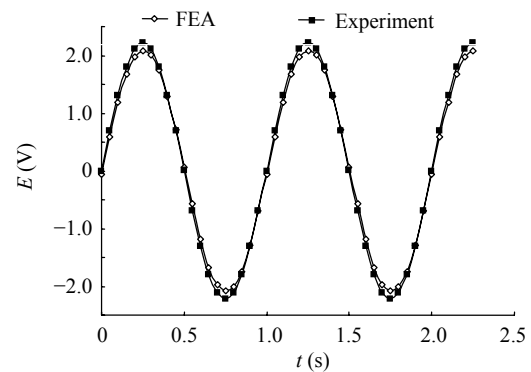


**Fig.8 No-load back EMF at the velocity of 51 mm/s**

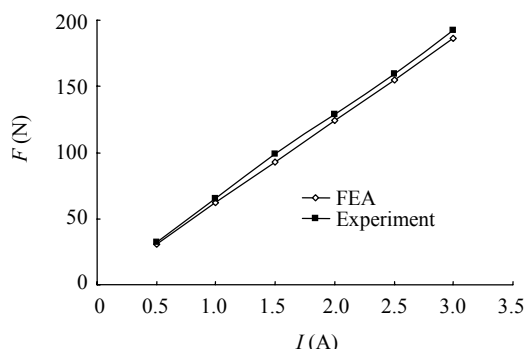


Fig.9 Thrust force with different currents

## CONCLUSION

Comparing the FEA results with the experimental results, the error is small and the FEA results are credible. The experimental results also prove that the performance of TPMLSM designed for driving the elevator door is very good. This novel elevator door system has the advantages of simple structure, low cost, high efficiency, rapid response and low acoustic noise, and thus is very suitable for manufacturing.

## References

- Bianchi, N., 2000. Analytical field computation of a tubular permanent-magnet linear motor. *IEEE Trans. on Magn.*, **36**(5):3798-3801. [doi:10.1109/20.908373]
- Bianchi, N., Bolognani, S., Tonel, F., 2001. Design Criteria of a Tubular Linear IPM Motor. Proc. IEEE Int. Electric Machines and Drives Conf., p.1-7.
- Bianchi, N., Bolognani, S., Corte, D., Tonel, F., 2003. Tubular linear permanent magnet motors: an overall comparison. *IEEE Trans. on Ind. Appl.*, **39**(2):466-475. [doi:10.1109/TIA.2003.809444]
- Jang, S.M., Choi, J.Y., Lee, S.H., Cho, S.K., Jang, W.B., 2003. Analysis of the Tubular Motor with Halbach and Radial Magnet Array. Proc. Int. Conf. on Electrical Machines and Systems, p.250-252.
- Lu, H.W., Zhu, J.G., Guo, Y.G., 2005. Development of a slotless tubular linear interior permanent magnet micro-motor for robotic applications. *IEEE Trans. on Magn.*, **41**(10):3988-3990. [doi:10.1109/TMAG.2005.855158]
- Lu, H.W., Zhu, J.G., Guo, Y.G., 2006. A Permanent Magnet Linear Motor for Micro Robots. Proc. Int. Conf. on Power Electronics and Drive Systems, p.590-595.
- Marignetti, F., Scarano, M., 1999. Analysis of PM Tubular Actuators. Proc. Int. Conf. on Electric Machines and Drives, p.440-442.
- Marignetti, F., Scarano, M., 2002. Comparative analysis and design criteria of permanent magnet tubular actuators. *Electr. Eng.*, **84**(5):255-264. [doi:10.1007/s00202-002-0127-5]
- Wang, J., Jewell, G.W., Howe, D., 1999. A general framework for the analysis and design of tubular linear permanent magnet machines. *IEEE Trans. on Magn.*, **35**(3):1986-2000. [doi:10.1109/20.764898]
- Wang, J., Jewell, G.W., Howe, D., 2001. Design optimization and comparison of tubular permanent magnet machine topologies. *IEE Proc.-Electr. Power Appl.*, **148**(5):456-464. [doi:10.1049/ip-epa:20010512]
- Wang, J., Howe, D., Jewell, G.W., 2003. Fringing in tubular permanent-magnet machines: Part I. Magnetic field distribution, flux linkage, and thrust force. *IEEE Trans. on Magn.*, **39**(6):3507-3516. [doi:10.1109/TMAG.2003.819463]
- Wang, J., Howe, D., Jewell, G.W., 2004. Analysis and design optimization of an improved axially magnetized tubular permanent-magnet machine. *IEEE Trans. on Energy Conv.*, **19**(2):289-295. [doi:10.1109/TEC.2004.827026]
- Zhao, G.X., Tang, R.Y., Chen, L.X., Lan, B., Liu, Y., 2006. Study and design of permanent magnet motor with ironless rotor. *Trans. China Electrotech. Soc.*, **21**(3): 58-61, 93.
- Zhou, Y., Shen, J.X., Ye, Y.Y., 2006. PSoC control of a LIM-driven elevator door. *Small & Special Electrical Machines*, **34**(5):22-23, 26 (in Chinese).
- Zhu, Z.Q., Xia, Z.P., Atallah, K., Jewell, G.W., Howe, D., 2000. Novel Permanent Magnet Machines Using Halbach Cylinders. Proc. Int. Power Electronics and Motion Control Conf., **2**:903-908.